



# Green Synthesis of $\text{TiO}_2$ Nanoparticles Using *Azadirachta Indica* with Multifunctional Bioactivity

Sidra Mamoor<sup>1</sup>, Atta Ullah<sup>1</sup>, Sulaiman Khan<sup>1</sup>, Waleed Ahsan Akber<sup>1</sup>, Shakir Ali<sup>1</sup>, Adil Sher<sup>2</sup>, Gauhar Rehman<sup>2</sup>, Khizar Hayat<sup>1</sup> and Said Karim Shah<sup>1,\*</sup>

<sup>1</sup> Department of Physics, Abdul Wali Khan University Mardan, Khyber Pakhtunkhwa 23200, Pakistan

<sup>2</sup> Department of Zoology, Abdul Wali Khan University Mardan, Khyber Pakhtunkhwa 23200, Pakistan

## Abstract

In this study, titanium dioxide nanoparticles ( $\text{TiO}_2$ -NPs) were synthesized via a green, cost-effective method using *Azadirachta indica* leaf extract as a natural capping and reducing agent. Characterization techniques including UV-vis, FTIR, XRD, SEM, EDX, and PL spectroscopy confirmed successful synthesis. UV-vis and FTIR confirmed surface functionalization by organic residues, while XRD revealed a well-crystalline anatase phase with average crystallite sizes of 42.2–54 nm. SEM analysis showed predominantly spherical particles (70–90 nm), and EDX confirmed high purity with only Ti and oxygen present. PL spectra exhibited emission peaks at 420, 468, 493, and 539 nm. The green  $\text{TiO}_2$ -NPs demonstrated multifunctional biomedical activities. In vitro anti-inflammatory assays showed significant human red blood cell membrane stabilization, with maximum inhibition of 74.7% and 71.3% in heat-induced hemolysis tests. Compared to diclofenac sodium standard,  $\text{TiO}_2$ -NPs achieved 87.3% and 76.3% inhibition at high concentrations.

Anti-diabetic assays revealed up to 71.4% inhibition of glucose uptake by yeast cells (vs. 86.6% for standard drugs), while glucose adsorption ranged from 0.45 to 7.3 mg/g. Antibacterial activity against Gram-positive (*Staphylococcus aureus*) and Gram-negative (*Escherichia coli*) strains showed inhibition zones of 22.2 mm and 21.2 mm, respectively, comparable to standard drugs (23.3 mm and 21.7 mm). These results highlight green  $\text{TiO}_2$ -NPs as promising candidates for biomedical applications.

**Keywords:** green  $\text{TiO}_2$ -NPs, *Azadirachta indica* leaf extract, anti-inflammatory, anti-diabetic, anti-bacterial efficacy.

## 1 Introduction

Nanotechnology is transformative in many industries, from energy and electronic to agriculture, textiles and food [1]. Its impact is especially significant in medicine, where it enables advances in targeted drug delivery, bio sensing, medical imaging, and wound healing gene therapy anti-bacterial treatments. NP features, such as their size, shape, biocompatibility, surface chemistry, surface-to-volume ratio, stability, reactivity, magnetic behavior, and low hazardous



Submitted: 25 July 2025

Accepted: 13 November 2025

Published: 18 February 2026

Vol. 1, No. 1, 2026.

[10.62762/JAB.2025.294658](http://dx.doi.org/10.62762/JAB.2025.294658)

\*Corresponding author:

Said Karim Shah

[saidkarim@awkum.edu.pk](mailto:saidkarim@awkum.edu.pk)

## Citation

Mamoor, S., Ullah, A., Khan, S., Akber, W. A., Ali, S., Sher, A., Rehman, G., Hayat, K., & Shah, S. K. (2026). Green Synthesis of  $\text{TiO}_2$  Nanoparticles Using *Azadirachta Indica* with Multifunctional Bioactivity. *Journal of Advanced Biomaterials*, 1(1), 10–25.

© 2026 by the Authors. Published by Institute of Central Computation and Knowledge. This is an open access article under the CC BY license (<https://creativecommons.org/licenses/by/4.0/>).



nature, can initiate the biomedical application [2–6]. Presently, huge amounts of NPs have been fabricated from silver (Ag), copper (Cu), zinc (Zn), titanium (Ti), alg (alginate), magnesium (Mg) and their oxides, respectively, via chemical, physical, and green synthesis techniques [7–13]. Metal and metal oxides NPs have predominantly application in the health and medicine sector, because they have approximately nil toxicity when interacting with the cells of mammals. Gold (Au)-NPs have the capability of damaging cancer cells with the assistance of heat generated by the light through a technique called photo thermal radiation therapy [14]. Silver (Ag) and ZnO-NPs possessed the strength to kill the bacterial cells, reduce inflammation, and facilitate the regeneration of tissues [15, 16]. Out of all these materials, TiO<sub>2</sub> has attracted great attention from researchers currently because of its unique characteristics, including high refractive index, stability, versatility, and biocompatibility. TiO<sub>2</sub> is a well-known n-type, wide-bandgap semiconductor with diverse applications, including as pigments, in photocatalysis and solar cells, in supercapacitors and coatings, and in medical products such as sunscreens and cosmetics [17–20]. It is normally existed in three fundamental forms like rutile, anatase and brookite. The anatase form of TiO<sub>2</sub> in the photocatalytic and cytotoxic domain are more efficient than the rutile form [21]. Existing research has reported that the mixed crystalline form of TiO<sub>2</sub> (rutile : anatase) in 1:4 ratio demonstrated prominence biomedical performance compared with the single crystal phase [22, 23]. Recently, researchers have reported the, anti-cancer, anti-skin infection, anti-viral, anti-fungal, and anti-microbial pharmacological potentials of TiO<sub>2</sub>-NPs [24–27]. TiO<sub>2</sub>-NPs produce reactive oxygen species such as OH and O<sub>2</sub><sup>–</sup> which can effectively damage the cancer and microbial cells [28]. The crystal structure and morphology TiO<sub>2</sub> NPs is very important for their use in biomedical applications and to achieve the desired functionality. Therefore, TiO<sub>2</sub>-NPs can be achieved in different shapes and morphologies depending the choice of synthesis route. Various synthesis methods have been reported in the literatures. Buraso et al. [29] synthesized TiO<sub>2</sub>-NPs by co-precipitation method and investigated their photocatalytic potential. Sadek et al. [30] manufactured TiO<sub>2</sub>-NPs adopting the method known as sol-gel. Arthi et al. [31], employed the solvothermal technique for TiO<sub>2</sub> nanostructures and fabricated dye-sensitized solar cells from them. Ansari et al. [32], used the biosynthesis method to synthesized TiO<sub>2</sub> NPs using *A. calamus* leaf extract

and investigated their anti-microbial and photolytic activities. Aravind et al. [33], used the extract of jasmine flowers in a green technique and efficiently fabricated TiO<sub>2</sub>-NPs and studied their multifunctional biomedical properties.

Diseases such as inflammation, bacterial infections, and diabetes are highly prevalent and necessitate the development of innovative and effective therapeutics. Inflammation is the body's immune system response to external injurious stimuli, including toxic or chemical irritants, pathogens, and cell damage, characterized by redness, swelling, pain, warmth, and loss of function [34, 35]. A small period of time of inflammation is called acute, which basically extends and converts into chronic inflammation [36]. Chronic inflammation performs an important character in the cellular remodeling and encourages a considerable amount of reactive oxygen species production and cell proliferation [36]. The enlargement of chronic inflammation leads to diseases including obesity, sugar, metabolic disorder, cardiac diseases, rheumatoid arthritis, and cancer [37].

A chronic disorder of carbohydrate breakdown that includes insufficient production of insulin or inability to respond appropriately to insulin, leading to higher glucose levels in the blood (refer as diabetes). It is the tenth leading cause of death worldwide [41]. Diabetes has been divided into three primary types, including gestational Diabetes, Type 1 Diabetes, and the most common Type, type 2 Diabetes [38, 39]. Long-lasting and untreated diabetes may cause microvascular and macrovascular problems that cause death and disability in diabetic humans [40]. International estimates reports that around 638.6 million people worldwide will live with suffering from diabetes by the year 2045 [42]. Diabetes has such an extremely dangerous consequence that researchers are eager to work hard and produce safe, efficient, and cost-effective medication to treat it precisely.

In this study, we present green synthesized TiO<sub>2</sub>-NPs using *Azadirachta indica* leaf extract for biomedical application. *Azadirachta indica*, which is also known as neem, is the evergreen, fast-growing, approximately 20-25m tall plant of the Meliaceae family and is native to the Indian subcontinent and Africa [43]. The Aza plant has historically served a vital part in therapeutics owing to more than 60 bioactive ingredients discovered in its leaves, seeds, flowers, and trunks, comprising nimbin, nimbidin, azadirachtin, nimbolinin, and many more [44].

The synthesized green  $\text{TiO}_2$ -NPs were characterized by XRD, SEM, EDX, FTIR, UV-VIS and PL to study their structural, morphological, elemental, Optical and functional group composition. Biomedical activities such in vitro anti-diabetic, anti-inflammatory and antibacterial activities using  $\text{TiO}_2$ -NPs were performed. In vitro assays revealed strong anti-inflammatory activity through effective stabilization of human red blood cell (HRBC) membranes, indicating their role in protecting cells against lysis under stress conditions. Simultaneously, anti-diabetic potential was validated via glucose adsorption assays, where the NPs exhibited significant glucose uptake efficiency. Moreover,  $\text{TiO}_2$ -NPs showed pronounced anti-bacterial effects against both Gram-positive and Gram-negative (E-coli & *Staphylococcus aureus*) strains, highlighting their broad spectrum antimicrobial action.

## 2 Materials and Methods

### 2.1 Materials

The fresh, healthy *Azadirachta indica* (Neem) leaves were obtained from M. Anis Nursery Farm, Guli Bagh, Mardan KPK, Pakistan. The chemicals isopropoxide ( $\text{C}_{12}\text{H}_{28}\text{O}_4\text{Ti}$ ), sodium hydroxide ( $\text{NaOH}$ ), sodium chloride ( $\text{NaCl}$ ), and glassware were purchased from Sigma Aldrich. The healthy blood for anti-inflammation activity was collected from a healthy individual following the standard protocol. The Department of Zoology, AWKUM provided the E. coli bacterial strain (ATCC8739) for antibacterial activity. The levofloxacin, metformin, and diclofenac

drugs were obtained from the Pharmacy Department, AWKUM. Furthermore, two-way ANOVA method is used for statistical analysis.

### 2.2 *Azadirachta indica* leave extract collection

The *Azadirachta indica* leaves were first resirised with tap water, then with distilled water. A total of 20g of leaves was added to 100mL of distilled water in a beaker and heated on hot plate at 60°C, for half an hour with continuous stirring. A yellowish *Azadirachta indica* extract was obtained which was stored at 4°C until further use in  $\text{TiO}_2$  synthesis.

### 2.3 Synthesis of $\text{TiO}_2$ -NPs

$\text{TiO}_2$ -NPs were synthesized with some modifications using the standard synthesis procedures [45]. In the very first step double-distilled water is used as solvent to prepare 0.1 M titanium isopropoxide. *Azadirachta indica* leaf extract was added drop wise to obtain a pH7. The solution was stirred at a constant frequency at 50°C for 4h. The dense yellowish solution was then resin with distilled water and ethanol for 10 min at 3000rpm three times using centrifugation. The obtained precipitate was kept in oven at 60°C for 60 min to dry. Finally, the samples were annealed at 450°C for 2h. Figure 1 shows synthesis flowchart of green  $\text{TiO}_2$  -NPs. The green  $\text{TiO}_2$  samples were synthesized by treating it with two different concentrations of *Azadirachta indica* extract (20mL & 30mL) respectively and pure  $\text{TiO}_2$  sample was prepared by synthetic route.

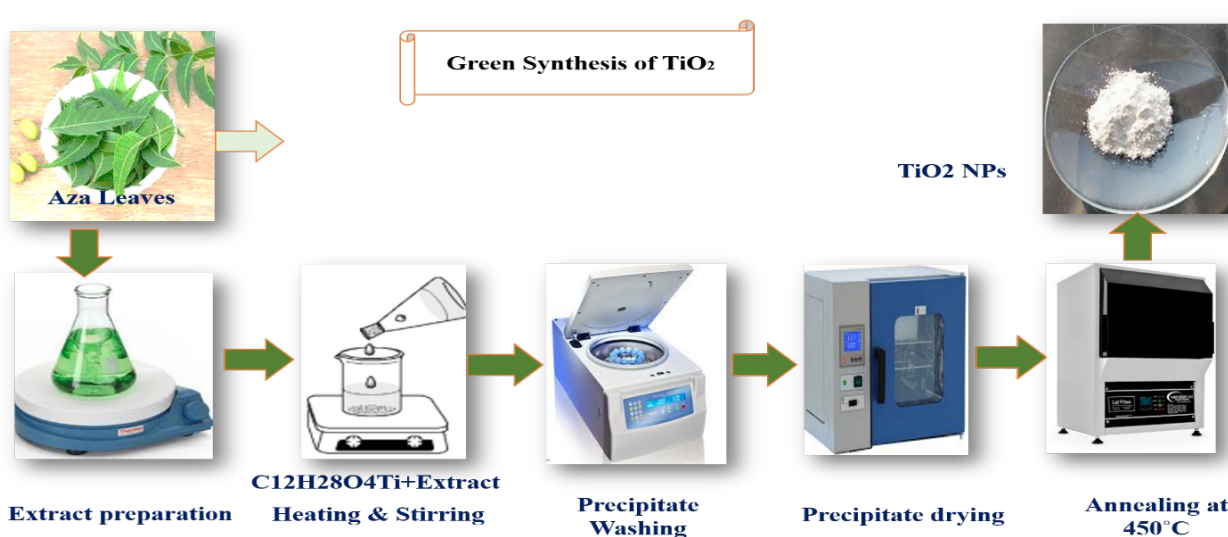


Figure 1. Flowchart of synthesis of  $\text{TiO}_2$ -NPs with the *Azadirachta indica* extract.

### 3 In vitro anti-inflammatory activity

#### 3.1 Suspension preparation for HRBC membrane stabilization assay

The anti-inflammatory potential of TiO<sub>2</sub>-NPs were examined implementing the HRBCs membrane stabilization assay. The fresh and healthy blood was obtained from an individual in good health in an EDTA tube who had not taken any medicines for 14 days. The blood was centrifuged many times for 20 min at ambient temperature at 4000rpm. The supernatant was discarded, and the pellet containing HRBCs was used. The normal saline solution 0.9% (w/v) was employed for washing the HRBCs. A 10% (v/v) suspension of RBCs has been prepared in normal saline solution. Then the 10% HRBC suspension in phosphate-buffered saline was prepared and treated with different concentrations (10μm/mL-70μm/mL) of TiO<sub>2</sub>-NPs, such as pure-TiO<sub>2</sub>, TiO<sub>2</sub>-20mL, TiO<sub>2</sub>-30mL and standard drug (diclofenac sodium). The HRBCs were later exposed to hypotonic saline (0.25–0.5% NaCl) to trigger hemolysis. The resultant mixture underwent incubation at 37°C for half an hour and was then centrifuged. The absorbance of the supernatant was determined using spectrometer at the wavelength (λ=540 nm). The percentage inhibition was calculated by using equation (1) [12].

$$\% \text{inhibition} = \frac{\text{Control absorbance} - \text{Treated absorbance}}{\text{Control absorbance}} \times 100 \quad (1)$$

#### 3.2 Suspension preparation for heat-induced hemolysis assay

To study the anti-inflammatory capability of pure-TiO<sub>2</sub>, TiO<sub>2</sub>-20mL, and TiO<sub>2</sub>-30mL, diclofenac sodium was tested in comparison with TiO<sub>2</sub> samples. A 10% HRBC suspension was prepared with TiO<sub>2</sub>-NPs and diclofenac sodium at various concentrations (10 μg/mL-70 μg/mL). To induce hemolysis, the resulting mixture was incubated at 54 °C for approximately 20 min. At room temperature, the reaction mixtures were allowed to cool down, and then the samples were centrifuged at 4000 rpm for 5 min. The absorbance was measured using a spectrometer at a wavelength λ = 540 nm, and the corresponding percentage inhibition was calculated using equation (2).

$$\% \text{inhibition rate} = \frac{\text{Control Absorbance} - \text{Treated absorbance}}{\text{Control absorbance}} \times 100 \quad (2)$$

#### 3.3 Suspension preparation for Glucose adsorption assay

To investigate the glucose adsorption potential of TiO<sub>2</sub>-NPs, an *in vitro* anti-diabetic assay for glucose adsorption was conducted. A 100 mL glucose solution (5–25 mM glucose) was prepared and mixed with the test samples, using 0.5 g of each TiO<sub>2</sub> sample. The resultant solution was then incubated at 37 °C for 1 h. The supernatant was separated by repeated centrifugation. Using a glucometer, the absorbance values G1 (before the reaction, representing initial glucose concentration) and G6 (after 6 h, representing final glucose concentration) were determined. The amount of adsorbed glucose was calculated using equation (3).

$$\text{Bounded Glucose} = \frac{G1 - G6}{\text{Control absorbance}} \times \text{Volume of sample} \quad (3)$$

#### 3.4 Suspension preparation for Glucose uptake by yeast cells

The aim of this experiment was to investigate the anti-diabetic potential of TiO<sub>2</sub>-NPs using an *in vitro* antidiabetic assay based on glucose uptake by yeast cells. Metformin was used as a standard drug for comparison with the tested samples.

Yeast cells were separated from the yeast solution through repeated centrifugation, and a colloidal suspension of yeast cells in distilled water was prepared. Test samples (TiO<sub>2</sub>-NPs) were dissolved in ethanol, and a glucose solution (5 mM, 1 mL) was also prepared. A mixture containing all three solutions was prepared and incubated for 30 min at 37 °C. Various concentrations (20–80 μg/mL) of TiO<sub>2</sub>-NPs and metformin were incubated under the same conditions.

Glucose uptake was measured before and after the experiment using a spectrometer at a wavelength of 520 nm. The percentage increase in glucose uptake was calculated using equation (4).

$$\% \text{ increase in glucose uptake} = \frac{\text{Abs(control)} - \text{Abs(sample)}}{\text{Abs(control)}} \times 100 \quad (4)$$

#### 3.5 In vitro antibacterial activity

The antibacterial activity of TiO<sub>2</sub> nanoparticles (TiO<sub>2</sub>-NPs) was evaluated using the agar well diffusion method against Gram-negative *E. coli* and

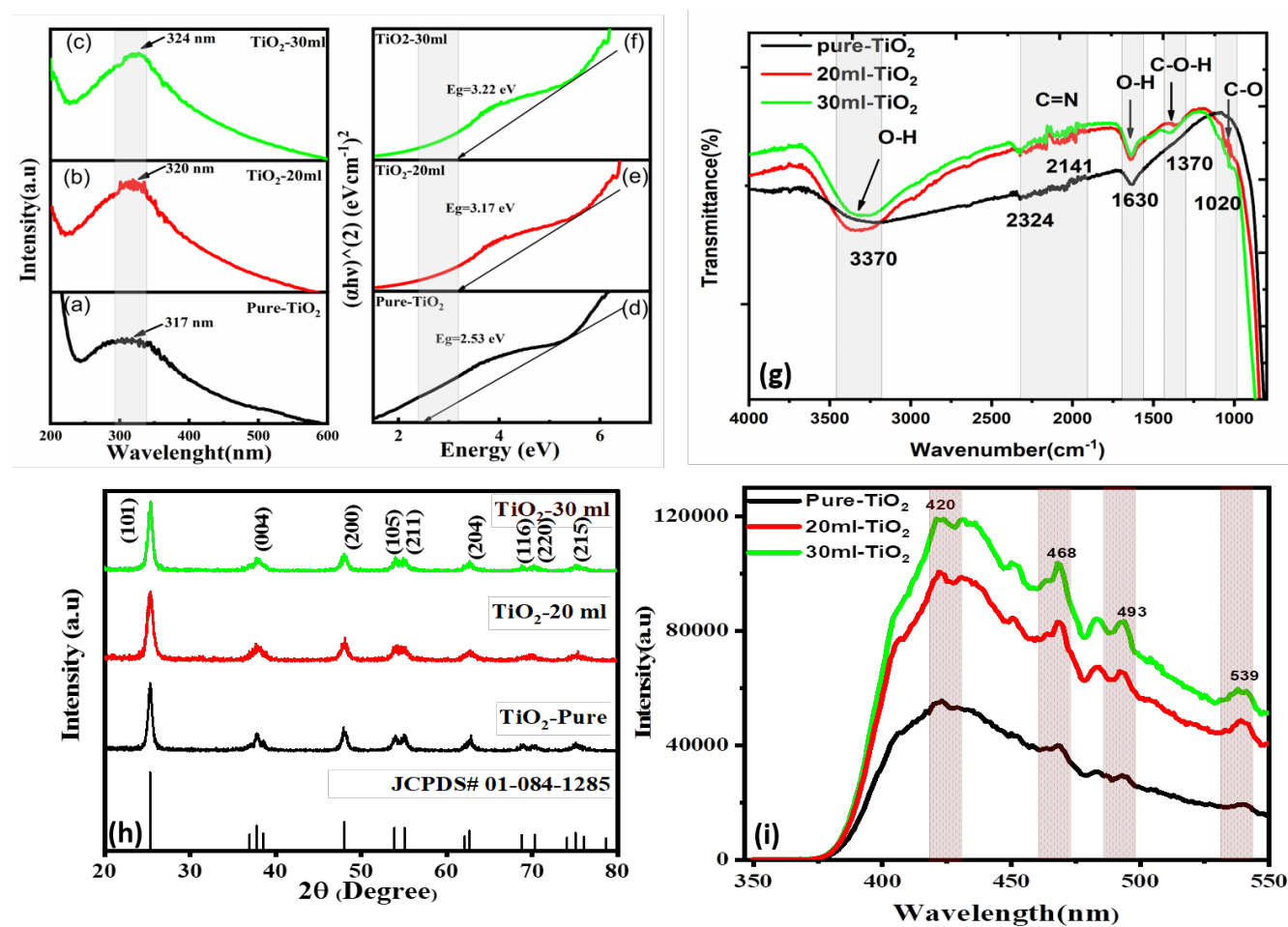


**Figure 2.** (a-c) shows UV-vis profiles of  $\text{TiO}_2$ -NPs, (d-f) shows bandgap profile of each sample, (g) shows FTIR spectra of  $\text{TiO}_2$ -NPs, (h) XRD pattern and (i) photoluminescence spectrum of  $\text{TiO}_2$ -NPs.

Gram-positive *S. aureus* bacterial strains, following the procedure described by Buraso et al. [29].

Sterile Mueller Hinton Agar (MHA) plates were prepared and inoculated with bacterial suspensions standardized to 0.5 McFarland. Approximately 100  $\mu\text{L}$  of each suspension was evenly spread over the agar surface. A sterile cork borer was then used to punch five wells, each 6 mm in diameter, into the agar.

For *E. coli*, three wells were filled with 50  $\mu\text{L}$  of  $\text{TiO}_2$  suspensions (pure  $\text{TiO}_2$ ,  $\text{TiO}_2$ -20 mL, and  $\text{TiO}_2$ -30 mL), one with the standard antibiotic levofloxacin (positive control), and one with 10% sterile DMSO (negative control). For *S. aureus*, separate plates were prepared, and two concentrations (30  $\mu\text{L}$  and 60  $\mu\text{L}$ ) of each  $\text{TiO}_2$  suspension (pure  $\text{TiO}_2$ ,  $\text{TiO}_2$ -20 mL, and  $\text{TiO}_2$ -30 mL) were tested.

The plates were incubated at 37 °C for 24 h. After incubation, the inhibition zone diameter of each well was measured in triplicate using a Vernier caliper to ensure precise and accurate results.

## 4 Results and discussions

The optical, structural and spectroscopic analysis of pure and green  $\text{TiO}_2$ -NPs samples provided a comprehensive insight into the extract induced modifications in the physiochemical behavior of the samples. UV-Vis absorption spectra as shown in Figure 2(a-c), which revealed a distinct redshift from 317 nm, 320 nm and 324 nm for pure, 20 mL and 30 mL samples respectively. It indicates enhanced visible light absorption and defect formation due to extract mediated surface modification in green and chemically synthesized  $\text{TiO}_2$ -NPs. This shift signifies improved photon harvesting ability and narrowed particle size distribution, which promote charge excitation and reactive oxygen species generation (ROS), crucial for anti-bacterial, anti-diabetic and anti-inflammatory mechanism [46, 47].

The corresponding Tauc's plots given in Figure 2(d-f), estimated optical bandgaps of 2.53 eV for pure, increasing to 3.17 and 3.22 eV for the 20 mL and 30 mL samples, suggesting extract assisted crystalline

refinement and organic functionalization that alter electronic transition [48].

FTIR spectra given in Figure 2(g) further confirmed the successful incorporation of phytochemicals from the extract showing characteristic O-H stretching around  $3370\text{ cm}^{-1}$ , C=O and C-O vibrations at  $1630$  and  $1020\text{ cm}^{-1}$  and C-N at  $2141\text{ cm}^{-1}$  [49]. These functional groups attached due to bioactive compounds such as phenols, terpenoids and alkaloids etc, which enhanced surface hydrophilicity and biocompatibility, enabling better bimolecular interactions of  $\text{TiO}_2$ -NPs in biomedical assays.

Furthermore, Figure 2(h) presents the XRD patterns of green-synthesized and chemically synthesized  $\text{TiO}_2$ -NPs. The XRD of  $\text{TiO}_2$  reported the reflective planes at Miller indices (101), (004), (200), (105), (211), (204), (116), (220), and (215) corresponding to the  $2\theta$  angle at  $25.2^\circ$ ,  $37.6^\circ$ ,  $47.9^\circ$ ,  $54.0^\circ$ ,  $54.9^\circ$ ,  $62.6^\circ$ ,  $68.7^\circ$ ,  $70.2^\circ$ , and  $75.0^\circ$ , respectively. The existence of sharp and intense peaks in the XRD of  $\text{TiO}_2$  revealed their well crystalline nature. The intensive peak (101) at  $25.2^\circ$   $2\theta$  value represents the  $\text{TiO}_2$  characteristic peak. The XRD of  $\text{TiO}_2$ -NPs matches well with JCPDS card no. (01-084-1285) and confirmed the anatase phase of  $\text{TiO}_2$ -NPs with tetragonal arrangement of atoms.

The average crystalline size was measured from XRD by Debye Scherer formula,

$$D = \frac{k\lambda}{\beta \cos \theta} \quad (5)$$

where  $\lambda$  is the wavelength of the X-ray,  $\beta$  represents the full width at half the maximum (FWHM) intensity,  $\theta$  is assigned for Bragg's angle, and  $k$  is called the Scherer constant. Equation (5) gives an average crystallite size of  $27.5\text{ nm}$  of  $\text{TiO}_2$ -NPs calculated from XRD peaks. The XRD of  $\text{TiO}_2$ -NPs did not show any shift or secondary peak.

Photoluminescence characterization was employed at room temperature, with  $350\text{ nm}$  exciton wavelength for the study of electronic structure and optical properties of prepared  $\text{TiO}_2$ -NPs. Figure 2(i) shows that the  $\text{TiO}_2$ -NPs exhibited several peaks in the PL spectra, showing an identical profile with only variation in the intensity levels. The visible peak at a wavelength of  $420\text{ nm}$  describes blue-violet emission observed in all three samples, indicating the self-trapped-electron-hole pair in the  $\text{TiO}_2$  nanostructures [50]. The emission peak located at  $468\text{ nm}$  corresponds to the emission of blue light might be associated with the transition of charged

entities at a higher level [51, 52]. The less intense and broad peaks at  $493\text{ nm}$  (blue-green region) and  $539\text{ nm}$  (green region) are assigned to the transition of electrons in the states that are formed due to the oxygen vacancies at the time of synthesis of  $\text{TiO}_2$  [53, 54]. The higher PL intensity in green synthesized  $\text{TiO}_2$ -NPs describes the greater electron-hole recombination rate as compared to chemically synthesized ones [40]. the phytochemicals (tannins, phenols, terpenoids, alkaloids and flavonoids etc) remains with  $\text{TiO}_2$  after treating with green extract play an active role in shaping its electronic structure. These organic compound act as stabilizing and reducing agents, which partially reduce  $\text{Ti}^{4+}$  to  $\text{Ti}^{3+}$  and create oxygen vacancies in the  $\text{TiO}_2$  lattice. Such defects are well known to serve as radiative recombination centers, where electrons and holes recombine with photon emission, giving rise to PL intensity. Additionally these organic residues from *Azadirachta indica* often bound to the  $\text{TiO}_2$  surface, introducing shallow surface states, that favor radiative over non radiative transition, this phenomena helps in smaller particle sizes and larger surface areas further confirming defect related and surface state emission [55–57]. Overall the enhanced PL intensity reflects the direct influence of phytochemicals, present in the extract treated samples which tailors optical properties.

The SEM micrographs of  $\text{TiO}_2$ -NPs given in Figure 3(a-c) exhibit highly agglomerated, roughly spherical NPs. The elemental compositions of  $\text{TiO}_2$ -NPs were revealed by EDX analysis. EDX reported exclusively the constituent elements of the prepared product such as Ti and Oxygen ( $\text{O}_2$ ) with no extra peaks of any other elements. The EDX profiles along with atomic and weight percentages of Ti and  $\text{O}_2$  are given Figure 3(e-f), The narrow and intense EDX peaks are defining the well-crystalline and highly pure nature of the prepared product. The EDX confirms a significant increase in the amount of oxygen in the resulting product, which may be due to the organic compounds present in the Aza extract mediating the increase. Moreover, The average particle size was calculated using the ImageJ software. The estimated particle sizes for pure,  $20\text{ mL-TiO}_2$ , and  $30\text{ mL-TiO}_2$  samples are  $91.8\text{ nm}$ ,  $84.1\text{ nm}$ , and  $72.4\text{ nm}$ , respectively. The corresponding histograms given in Figure 4(a-c) highlight the numerical details on the distribution of  $\text{TiO}_2$ -NPs. The particle sizes of the synthesized NPs are significantly decreased with the incorporation of extract, which is evidence of the capping and reducing capability of phytochemicals in

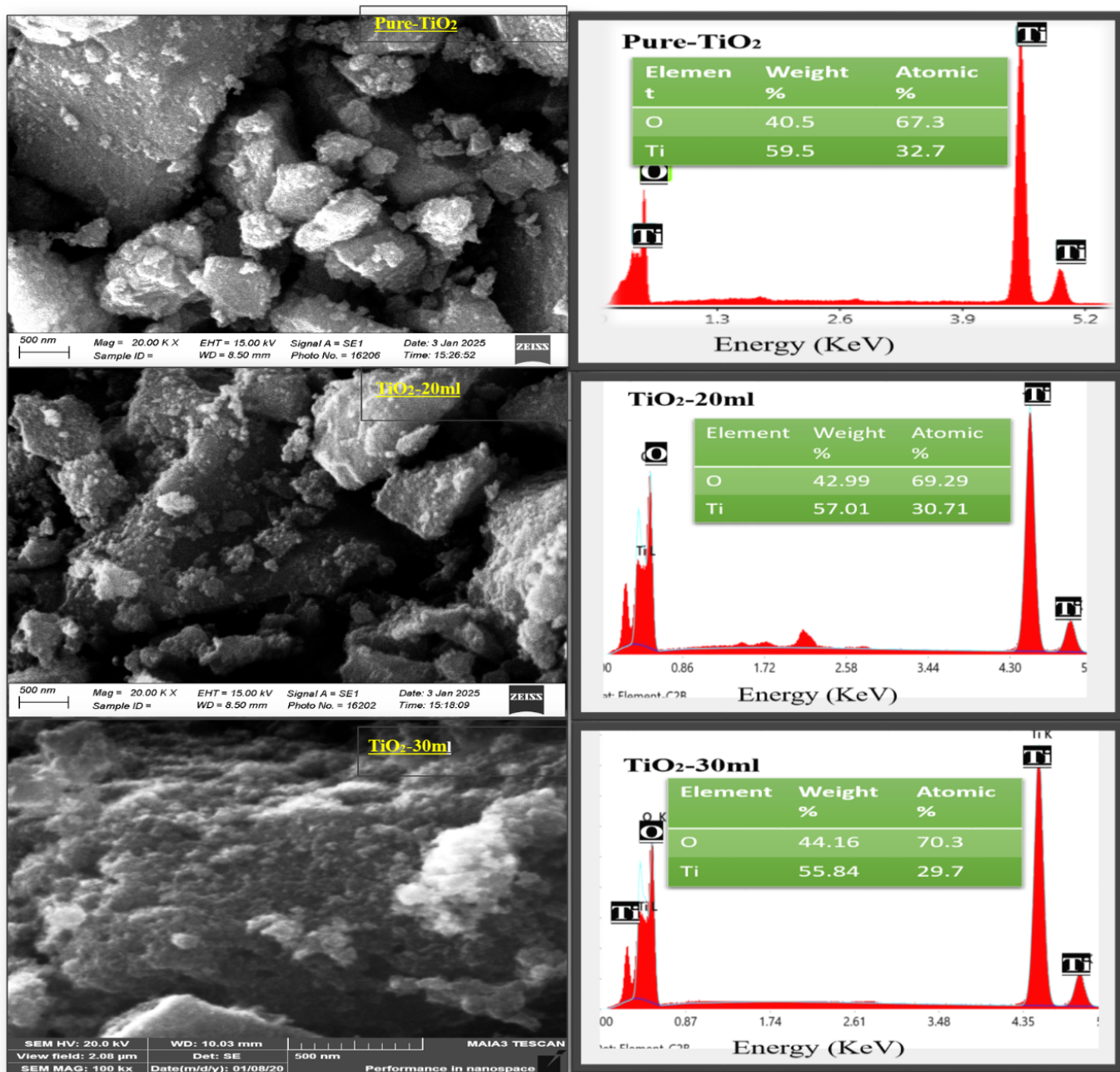


**Figure 3.** SEM micrographs of  $\text{TiO}_2$ -NPs and corresponding nanoparticles particles distributions histograms & EDX profiles of  $\text{TiO}_2$ -NPs.

the Aza leaves extract.

#### 4.1 In vitro anti-inflammatory Activity

##### 4.1.1 HRBC membrane stabilization assay

The anti-inflammatory potential of  $\text{TiO}_2$ -NPs and the standard drug was tested in seven concentrations from  $10\mu\text{g}/\text{mL}$  to  $70\mu\text{g}/\text{mL}$ . The activity has reported a dose-dependent behavior of the tested sample, as shown in Figure 5(a). At a concentration of  $70\mu\text{g}/\text{mL}$ , the four samples (pure, 20mL, 30mL, and standard) displayed the maximum inhibition and

the lowest at  $10\mu\text{g}/\text{mL}$ . The maximum inhibition percentage shown by pure, 20mL, 30mL and standard are 54.6%, 69.7%, 74.7% and 87.3% respectively, where the minimum inhibition for each tested sample is 5.6% 10.9%, 15%, and 20.2%. The green synthesized  $\text{TiO}_2$ -NPs showed a significant anti-inflammatory potential in contrast to the standard drug used in this study. Notably,  $\text{TiO}_2$ -30mL suggests that increased extract volume during synthesis enhances bioactivity of  $\text{TiO}_2$ -NPs, likely due to improved surface functionalization and phytochemical

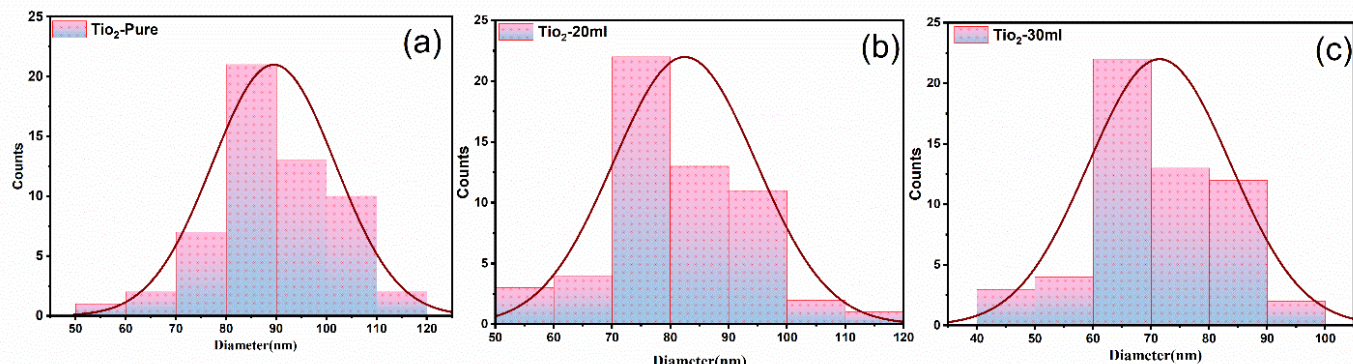


**Figure 4.** Histograms of  $\text{TiO}_2$ -NPs, particle size calculated from SEM micrographs using ImageJ software.

capping. Specifically, phenolics and flavonoids stabilize lysosomal and RBC membranes, suppressing the leakage of inflammatory mediators. They also downregulate lipoxygenase and cyclooxygenase enzymes, reducing the production of leukotrienes and prostaglandins [58]. The high amount of these organic residues might be the reason why the 30mL sample closely followed the standard drug result in each concentration and shows effective anti-inflammatory behavior. These findings align with the prior studies reported on green synthesized  $\text{TiO}_2$ -NPs using as an anti-inflammation agent [59, 60].

#### 4.1.2 HRBC heat induced hemolysis

The high temperature treatment caused the hemolysis in human red blood cells. To inhibit the lysis of the cell membrane,  $\text{TiO}_2$ -NPs and a standard drug were used. In this activity, seven different concentrations from  $10\mu\text{g}/\text{mL}$  to  $70\mu\text{g}/\text{mL}$  of each sample were tested. The hemoglobin amount was measured with a spectrometer. The maximum inhibition% demonstrated by 70 concentrations in a standard, 30mL, 20mL, and pure samples are 76.3%, 71.3%, 62.3%, 58.3% respectively and the minimum inhibition% reported in 10 concentrations are 18.1%, 14.2%, 7.55%, and 3.6%. The  $\text{TiO}_2$ -30mL sample effectively stabilized the HRBC membrane in contrast with the other two samples and closely followed the standard drug in each concentration, as shown in Figure 5(b). Additionally, a dose-dependent anti-inflammatory potential was noticed by each sample, dominated by 30mL- $\text{TiO}_2$ , confirming the role of high amount of organic residues present on the surface of the  $\text{TiO}_2$  framework. In conclusion, the green synthesized  $\text{TiO}_2$ -NPs reported dominant anti-inflammatory activity over pure ones, which signifies the anti-inflammatory nature of the extract used as a capping and stabilizing solvent for the synthesis of  $\text{TiO}_2$  [61].

## 4.2 In vitro Anti-diabetic activity

### 4.2.1 Glucose adsorption assay

To study the Glucose adsorption capability of  $\text{TiO}_2$ -NPs, Various concentrations from (5-30mM) of  $\text{TiO}_2$  NPs (30mL- $\text{TiO}_2$ , 20mL- $\text{TiO}_2$ , and pure- $\text{TiO}_2$ ) were tested in the glucose adsorption assay. The activity demonstrated a maximum glucose adoption percentage at 30mM concentration are 7.5, 6.55, and 5 for 30mL- $\text{TiO}_2$ , 20mL- $\text{TiO}_2$  and pure- $\text{TiO}_2$ -NPs respectively, where in comparison the minimum adsorption percentages exhibited by  $\text{TiO}_2$  samples at 5mM concentration, numerically equal to 1.8, 1.3 and 0.4 respectively as displayed in Figure 6(a). Furthermore, the findings of the activity showcased a dose-dependent increase, as glucose amount effectively influenced the adsorption percentage. Similar trends have been reported in prior studies, where phytochemically functionalized metal oxide-NPs, demonstrated improved glucose uptake due to enhanced surface activity and affinity for glucose molecules [62, 63].

### 4.2.2 Glucose uptake by yeast cells

The anti-diabetic properties of  $\text{TiO}_2$ -NPs were investigated with the assay of glucose uptake by yeast cells. The assay registered a dose-dependent increase in uptake efficiency in all tested samples with significant findings. Moreover, numerically, the maximum inhibition was demonstrated by each sample at the maximum concentration  $70\mu\text{g}/\text{mL}$  and the minimum was reported in the minimum  $10\mu\text{g}/\text{mL}$  concentration, as shown in Figure 6(b). The standard drug, 30mL- $\text{TiO}_2$ , 20mL- $\text{TiO}_2$ , and pure- $\text{TiO}_2$  displayed the maximum inhibition of 86.6%, 71.4%, 59.7%, and 52.65%, respectively, and the minimum inhibition of 17.6%, 12.5%, 8.67%, and 5.54%. The findings of the activity revealed that  $\text{TiO}_2$ -NPs and standard drug efficiently control the rate of glucose transport in the yeast cells in a

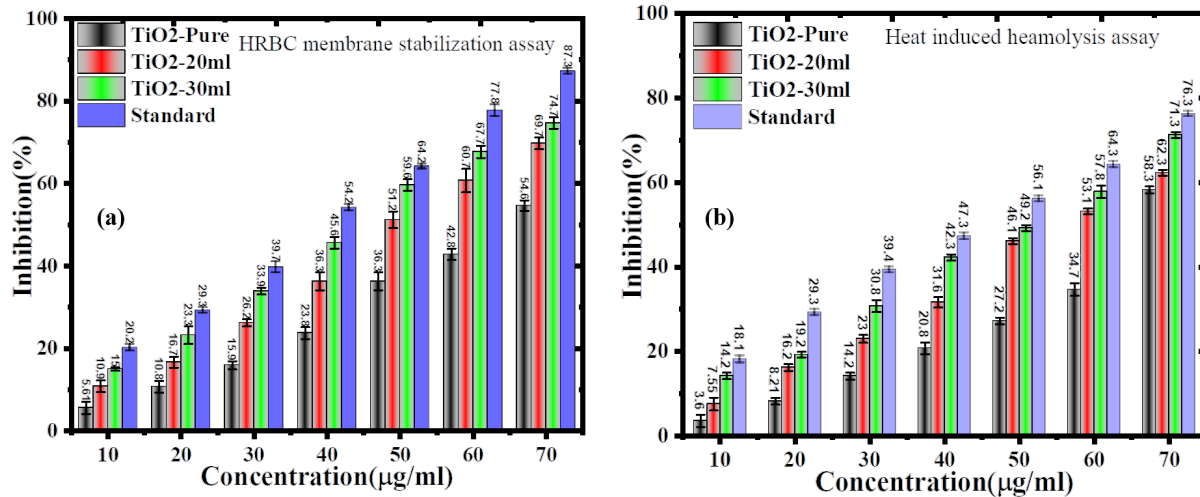


**Figure 5.** Anti-inflammatory activities. (a) HRBC membrane stabilization and (b) Heat induced haemolysis assay) of TiO<sub>2</sub>-NPs.

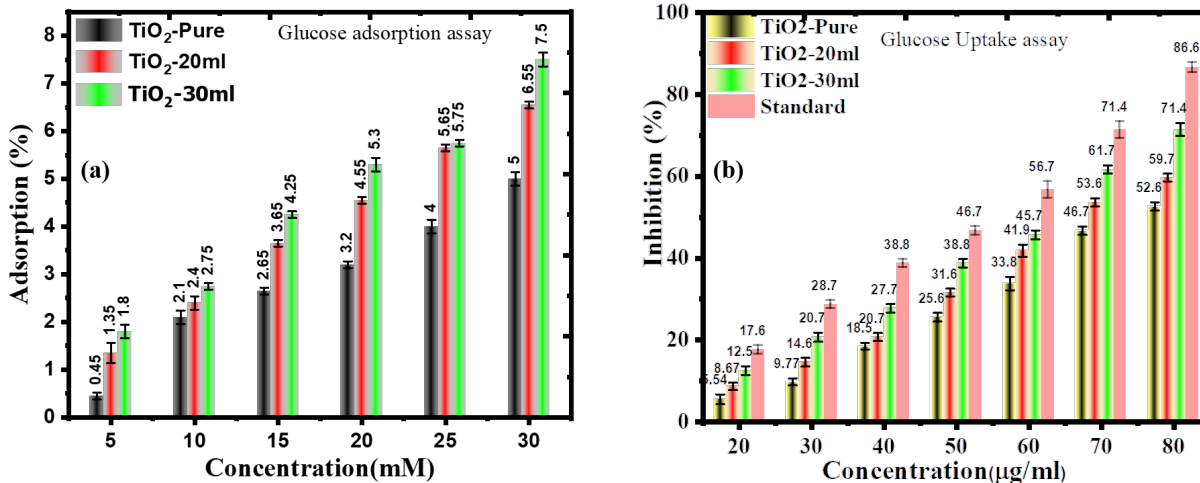


**Figure 6.** In vitro anti-diabetic activities of TiO<sub>2</sub>, including (a) Glucose adsorption assay and (b) Glucose uptake by yeasts cells.

dose-dependent pattern (especially 30mL extract). These enhanced results are attributed to the hydroxyl, carbonyl and phenolic groups which form hydrogen binds with glucose molecules, facilitating adsorption on the nanoparticle surface, moreover terpenoids and flavonoids are reported to enhance glucose uptake (cellular) by stimulating glucose transporter pathways and enhancing insulin mimetic activity [64]. Overall green-synthesized TiO<sub>2</sub>-NPs demonstrated relatively good results as compared to pure ones synthesized through chemical route because of the organic residues (phytochemicals) in the green extract treated samples.

### 4.3 Anti-bacterial activity

The antibacterial activity of TiO<sub>2</sub>-Samples was evaluated against gram positive *S. aureus* bacterial Strain using the agar well diffusion method, with test concentrations of 30  $\mu\text{L}$  and 60  $\mu\text{L}$  of each TiO<sub>2</sub> sample alongside a standard drug (levofloxacin). All samples exhibited distinct inhibition zones, confirming their antibacterial efficacy against *S. aureus*. Pure TiO<sub>2</sub>, TiO<sub>2</sub>-20 mL, and TiO<sub>2</sub>-30 mL effectively inhibited bacterial growth within their respective zones. At 60  $\mu\text{L}$ , Pure TiO<sub>2</sub> showed an inhibition zone of 17.84 mm, TiO<sub>2</sub>-20 mL exhibited 19.33 mm, and TiO<sub>2</sub>-30 mL demonstrated the highest activity with 22 mm,

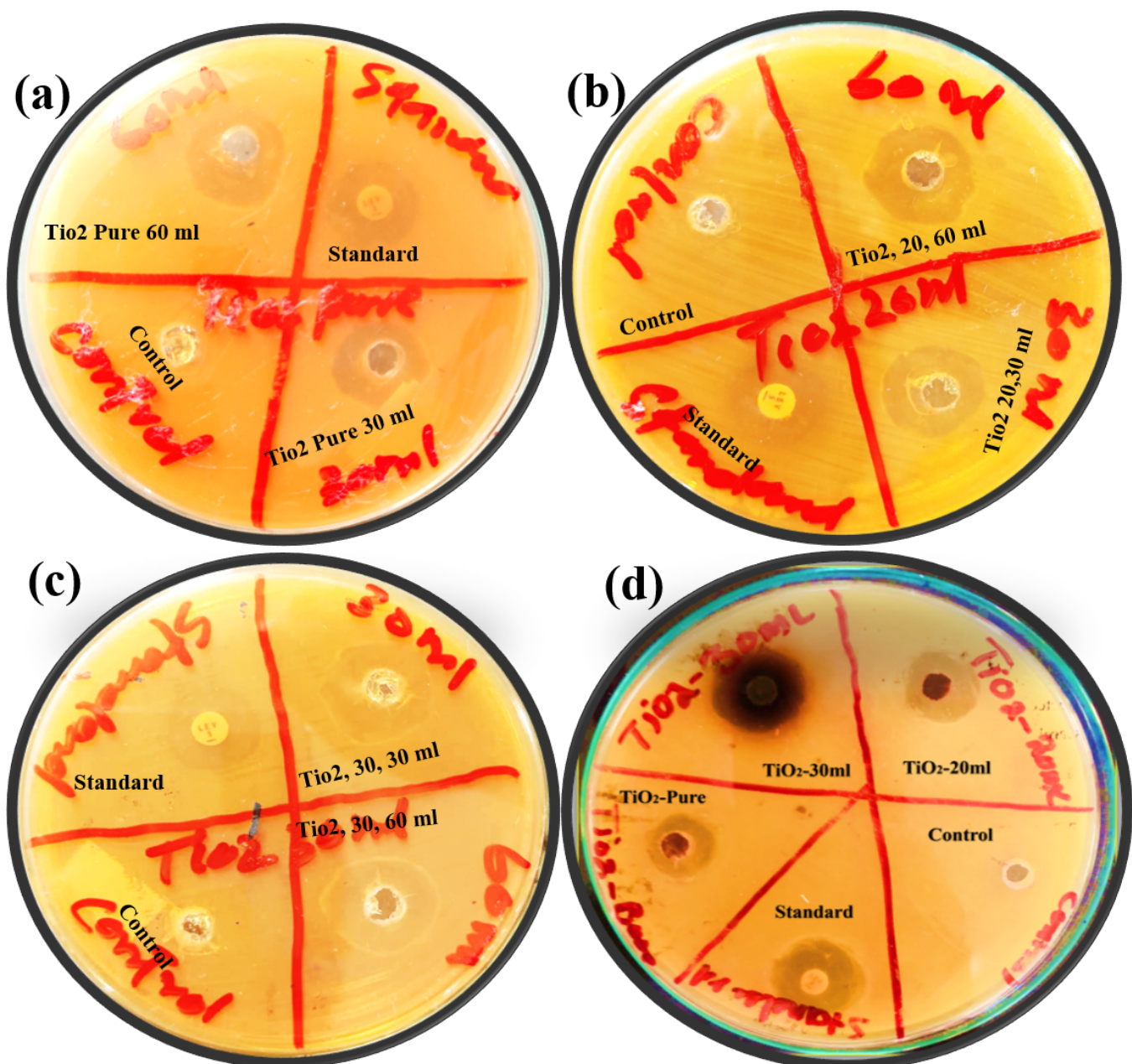


**Figure 7.** The well diffusion activity of TiO<sub>2</sub>-NPs against both gram positive bacteria, *S. aureus* (a-c) anti-bacterial response of each sample TiO<sub>2</sub>-pure, TiO<sub>2</sub>-20mL and TiO<sub>2</sub>-30mL at two different concentrations 30mL and 60 mL with standard levofloxacin and (d) shows inhibition zones of TiO<sub>2</sub> samples against gram negative *E.coli*.

whereas the standard drug shown a zone of 23.33 mm, given in Figure 8(b), Measurements were recorded using a Vernier caliper. The results highlight the dose-dependent antibacterial potential of TiO<sub>2</sub>-NPs, with TiO<sub>2</sub>-30 mL displaying comparable or superior activity to the reference drug, suggesting that TiO<sub>2</sub>

may serve as a promising antibacterial candidate antibacterial efficacy of TiO<sub>2</sub>-NPs and the standard drug was studied employing the Furthermore, against gram negative bacteria *E. coli*, a 50 $\mu$ L dose of each TiO<sub>2</sub> sample and reference drug is used in the test. The activity showed clear inhibition zones, confirming

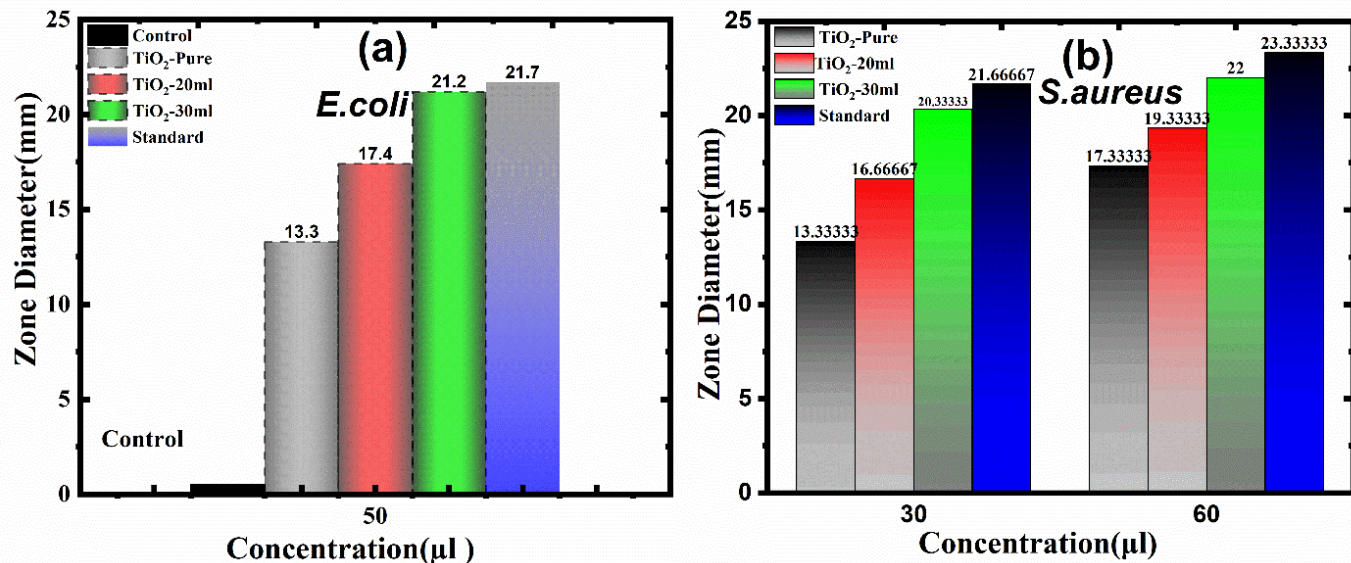


**Figure 8.** Zone diameter calculated using Vernier caliper (a) against *E. coli* at 50  $\mu\text{l}$  concentration, (b) shows the zone diameter against *S. aureus* bacteria at two different concentration 30 and 60  $\mu\text{l}$ .

**Table 1.** Comparative analysis of anti-bacterial activities of TiO<sub>2</sub>-NPs.

TiO <sub>2</sub> Synthesis routes	NP's Size (nm)	Tested bacteria	Volume ( $\mu\text{l}$ )	Inhibited Zone (mm)	Antimicrobial method	Medium used	Ref.
Electromagnetic synthesis (Pure TiO <sub>2</sub> )	25-30 (TEM)	<i>E. coli</i>	50	10.5	Well-diffusion method	Nutrient agar	[68]
Solution casting (Chitosan-TiO <sub>2</sub> composite)	30	<i>E. coli</i>	100	9.86	Well-diffusion method	Nutrient agar	[69]
Sol gel (Pure TiO <sub>2</sub> )	68 (SEM)	<i>S. aureus</i>	100	16	Disc- diffusion method	Muller-Hin-ton Agar	[70]
Sol gel(Pure TiO <sub>2</sub> )	68 (SEM)	<i>E. coli</i>	100	14	Disc- diffusion method	Muller-Hin-ton Agar	-
Green NPs (Azadirachta indica)	15-50 (TEM)	<i>S. aureus</i>	66	18	Well-diffusion method	Muller-Hin-ton Agar	[71]
Green synthesis ( <i>Psidium guajava</i> )	33 (FESEM)	<i>S. aureus</i>	20	25	Disc- diffusion method	Muller-Hin-ton Agar	[72]
TiO <sub>2</sub> (Lebedouria revolute)	47	<i>B. cereus</i>	60	4	Well-diffusion method	Nutrient Agar	[73]
Sol-gel (Pure TiO <sub>2</sub> )	78 (FESEM)	<i>E. coli</i> & <i>S. aureus</i>	50 30-60	17.413-17	Well-diffusion method	Nutrient Agar	This-work
Sol-gel- <i>Azadirachta indica</i> - 20mL-TiO <sub>2</sub>	72 (FESEM)	<i>E. coli</i> & <i>S. aureus</i>	50 30-60	21.216-19	Well-diffusion method	Nutrient Agar	This-work
Sol-gel- <i>Azadirachta indica</i> -30mL-TiO <sub>2</sub>	63 (FESEM)	<i>E. coli</i> & <i>S. aureus</i>	50 30-60	21.720-22	Well-diffusion method	Nutrient Agar	This-work

dose independent but extract enhanced antibacterial efficacy against *E. coli*, of the TiO<sub>2</sub>-NPs. They have effectively reduced or inhibited the growth of the *E. coli* bacterial strain in their corresponding zones. The affected zone diameter of the standard drug was measured using Vernier caliper, is to be 21.7mm; closely followed by 30mL sample at 21.2 mm, as shown in Figure 8(a), indicating comparable antibacterial activity. Hence such a close characteristic with the standard drug(levofloxacin) makes TiO<sub>2</sub> a potential anti-bacterial candidate in the field of biomedicine. Additionally, TiO<sub>2</sub>-20mL and the pure samples showed 17.4 mm and 13.3 mm inhibited zone diameters, respectively, as shown in Figure 7(d). the surface-bound phytochemicals, not only stabilize NPs but also impart additional bioactivity. These compounds enhances membrane

interaction, reactive oxygen species generation, and bacterial membrane disruption [65, 66]. The strong anti-bacterial response in this work is resulted from the synergism of phytochemicals mainly (terpenoids, tannins) and TiO<sub>2</sub> generated ROS. ROS directly damages microbial membranes while phytochemicals disrupt cell wall integrity, induce protein leakage and inhibit enzyme activity. This dual mechanism explains strong bacterial inhibition zones in the tested samples. Similar findings were reported on green synthesized TiO<sub>2</sub>-NPs which exhibited effective bactericidal effects due to ROS-mediated membrane damage. Another study emphasized the role of biological agents, which enhance their affinity in anti-bacterial effects [67]. Thus, the near-equivalent inhibition by the 30mL sample to that of the standard drug underscores the potential of green-synthesized

TiO<sub>2</sub>-NPs as an effective and sustainable anti-bacterial agent, particularly in biomedical and health care applications. Table 1 shows the comparative analysis of TiO<sub>2</sub>-NPs synthesis with different route and with different particle sizes.

## 5 Conclusion

In this study, TiO<sub>2</sub>-NPs were successfully synthesized via a green synthesis approach using the *Azadirachta indica* leaf extract, as a reducing agent. The elemental, structural, morphological, and optical properties of the synthesized green TiO<sub>2</sub>-NPs were characterized using UV, FTIR, XRD, EDX, SEM, and PL techniques. XRD confirmed the well-crystalline anatase phase, with average crystallite size ranging from 42nm to 55nm. SEM shows the spherically shaped agglomerated particles with average size of 70nm to 90nm. EDX confirm the Ti and oxygen at different ratios, with no other impurities. Optically visible light emission green TiO<sub>2</sub>-NPs observed at 420nm, 468nm, 493nm, and 539 nm. The biomedical activities, such as anti-inflammatory, anti-diabetic, and anti-bacterial activities, of the prepared green TiO<sub>2</sub>-NPs were conducted. In vitro anti-inflammatory investigation (HRBC membrane stabilization and heat-induced hemolysis) of TiO<sub>2</sub>-NPs reported a maximum of 74.7% and 71.3% inhibition in comparison with 87.3% and 76.3% inhibition of the standard drug, respectively. Furthermore, TiO<sub>2</sub>-NPs demonstrated 71.4% glucose uptake in yeast cells, in contrast to the standard drug, which displayed 86.6% in the in vitro anti-diabetic activity. The TiO<sub>2</sub>-NPs (30mL) showed a maximum of 6.55 glucose adsorption and a minimum of 0.45 in pure TiO<sub>2</sub>. The anti-bacterial activity using well diffusion methods, displayed a well-matched, well-aligned result with the reference drug. Compared to reference drug (an inhibition of 21.7 mm), the green TiO<sub>2</sub>-NPs (30mL) showed a slightly larger inhibition zone of 21.2 mm, indicating their comparable antibacterial efficacy. These findings validate the potential of the green TiO<sub>2</sub>-NPs as a multifunctional biomedical agent to treat diabetes, inflammation, and bacterial infections, providing a sustainable alternative to chemically produced Nano medicine.

## Data Availability Statement

Data will be made available on request.

## Funding

This work was supported by the Higher Education Department of Khyber Pakhtunkhwa

under Project ID 3118, through Grant PMU/1-22/HEREF/2014-15/Vol-VIII/7294.

## Conflicts of Interest

The authors declare no conflicts of interest.

## AI Use Statement

During the preparation of this work, the author(s) used ChatGPT to assist with English language improvements. The author(s) reviewed and edited the content as necessary and take(s) full responsibility for the final version of the publication.

## Ethical Approval and Consent to Participate

All procedures involving human participants were approved by the Institutional Ethical Review Committee of Abdul Wali Khan University, Mardan, Pakistan and conducted in accordance with institutional ethical and biosafety guidelines. Informed consent was obtained from a healthy adult blood donor prior to sample collection.

## References

- [1] Saritha, G. N. G., Anju, T., & Kumar, A. (2022). Nanotechnology-Big impact: How nanotechnology is changing the future of agriculture?. *Journal of Agriculture and Food Research*, 10, 100457. [\[CrossRef\]](#)
- [2] Kurul, F., Turkmen, H., Cetin, A. E., & Topkaya, S. N. (2025). Nanomedicine: How nanomaterials are transforming drug delivery, bio-imaging, and diagnosis. *Next Nanotechnology*, 7, 100129. [\[CrossRef\]](#)
- [3] Joseph, T. M., Kar Mahapatra, D., Esmaeili, A., Piszczyk, Ł., Hasanin, M. S., Kattali, M., ... & Thomas, S. (2023). Nanoparticles: taking a unique position in medicine. *Nanomaterials*, 13(3), 574. [\[CrossRef\]](#)
- [4] Sim, S., & Wong, N. K. (2021). Nanotechnology and its use in imaging and drug delivery. *Biomedical reports*, 14(5), 42. [\[CrossRef\]](#)
- [5] Altammar, K. A. (2023). A review on nanoparticles: characteristics, synthesis, applications, and challenges. *Frontiers in Microbiology*, 14, 1155622. [\[CrossRef\]](#)
- [6] Khan, I., Saeed, K., & Khan, I. (2019). Nanoparticles: Properties, applications and toxicities. *Arabian journal of chemistry*, 12(7), 908-931. [\[CrossRef\]](#)
- [7] Hasan, S. (2015). A review on nanoparticles: their synthesis and types. *Res. J. Recent Sci*, 2277, 2502.
- [8] Ealia, S. A. M., & Saravanakumar, M. P. (2017, November). A review on the classification, characterisation, synthesis of nanoparticles and their application. In *IOP conference series: materials*

science and engineering (Vol. 263, No. 3, p. 032019). IOP Publishing. [\[CrossRef\]](#)

[9] Khan, Y., Sadia, H., Ali Shah, S. Z., Khan, M. N., Shah, A. A., Ullah, N., ... & Khan, M. I. (2022). Classification, synthetic, and characterization approaches to nanoparticles, and their applications in various fields of nanotechnology: A review. *Catalysts*, 12(11), 1386. [\[CrossRef\]](#)

[10] Rahman, A., Rehman, G., Shah, N., Hamayun, M., Ali, S., Ali, A., ... & Alrefaei, A. F. (2023). Biosynthesis and characterization of silver nanoparticles using *Tribulus terrestris* seeds: Revealed promising antidiabetic potentials. *Molecules*, 28(10), 4203. [\[CrossRef\]](#)

[11] Ahmad, I., Khan, M. N., Hayat, K., Ahmad, T., Shams, D. F., Khan, W., ... & Shah, S. K. (2024). Investigating the antibacterial and anti-inflammatory potential of polyol-synthesized silver nanoparticles. *ACS omega*, 9(11), 13208-13216. [\[CrossRef\]](#)

[12] Ullah, A., Sadiq, A., Usman, M., Ahmad, I., Sher, A., Rehman, G., ... & Gunnella, R. (2025). Facile synthesis of zinc-based Prussian blue analogue (Zn-PBAs) for supercapacitor and biomedical applications. *Sustainable Materials and Technologies*, 44, e01357. [\[CrossRef\]](#)

[13] Khan, S., Ullah, A., Ahmad, I., Sher, A., Rehman, G., Hayat, K., ... & Gunnella, R. (2025). Therapeutic potential of green-synthesized ZnO from *Azadirachta indica*: a study on anti-diabetic, anti-inflammatory, and anti-bacterial activities. *Journal of Sol-Gel Science and Technology*, 116(2), 1581-1596. [\[CrossRef\]](#)

[14] Babaei, A., Mousavi, S. M., Ghasemi, M., Pirbonyeh, N., Soleimani, M., & Moattari, A. (2021). Gold nanoparticles show potential in vitro antiviral and anticancer activity. *Life Sciences*, 284, 119652. [\[CrossRef\]](#)

[15] Zahoor, S., Sheraz, S., Shams, D. F., Rehman, G., Nayab, S., Shah, M. I. A., ... & Khan, W. (2023). Biosynthesis and Anti-inflammatory Activity of Zinc Oxide Nanoparticles Using Leaf Extract of *Senecio chrysanthemoides*. *BioMed research international*, 2023(1), 3280708. [\[CrossRef\]](#)

[16] Nikolopoulou, S. G., Boukos, N., Sakellis, E., & Efthimiadou, E. K. (2020). Synthesis of biocompatible silver nanoparticles by a modified polyol method for theranostic applications: Studies on red blood cells, internalization ability and antibacterial activity. *Journal of Inorganic Biochemistry*, 211, 111177. [\[CrossRef\]](#)

[17] Zhao, Y., Li, C., Liu, X., Gu, F., Jiang, H., Shao, W., ... & He, Y. (2007). Synthesis and optical properties of TiO<sub>2</sub> nanoparticles. *Materials Letters*, 61(1), 79-83. [\[CrossRef\]](#)

[18] Pavithra, S., Bessy, T. C., Bindhu, M. R., Venkatesan, R., Parimaladevi, R., Alam, M. M., ... & Umadevi, M. (2023). Photocatalytic and photovoltaic applications of green synthesized titanium oxide (TiO<sub>2</sub>) nanoparticles by *Calotropis gigantea* extract. *Journal of Alloys and Compounds*, 960, 170638. [\[CrossRef\]](#)

[19] Ismail, W., Ibrahim, G., Atta, H., Sun, B., El-Shaer, A., & Abdelfatah, M. (2024). Improvement physical and photoelectrochemical properties of TiO<sub>2</sub> nanorods toward biosensor and optoelectronic applications. *Ceramics International*, 50(10), 17968-17976. [\[CrossRef\]](#)

[20] Chun Chen, P., Chon Chen, C., & Hsun Chen, S. (2017). A review on production, characterization, and photocatalytic applications of TiO<sub>2</sub> nanoparticles and nanotubes. *Current Nanoscience*, 13(4), 373-393. [\[CrossRef\]](#)

[21] Diebold, U. (2003). Structure and properties of TiO<sub>2</sub> surfaces: a brief review. *Applied Physics A*, 76(5), 681-687. [\[CrossRef\]](#)

[22] Jafari, S., Mahyad, B., Hashemzadeh, H., Janfaza, S., Gholikhani, T., & Tayebi, L. (2020). Biomedical applications of TiO<sub>2</sub> nanostructures: recent advances. *International Journal of Nanomedicine*, 15, 3447-3470. [\[CrossRef\]](#)

[23] Akakuru, O. U., Iqbal, M. Z., Saeed, M., Liu, C., Paosen, S., & Jiang, X. (2020). TiO<sub>2</sub> nanoparticles: properties and applications. In *TiO<sub>2</sub> Nanoparticles* (pp. 1-66). Elsevier. [\[CrossRef\]](#)

[24] Ziental, D., Czarczynska-Goslinska, B., Mlynarczyk, D. T., Glowacka-Sobotta, A., Stanisz, B., Goslinski, T., & Sobotta, L. (2020). Titanium dioxide nanoparticles: prospects and applications in medicine. *Nanomaterials*, 10(2), 387. [\[CrossRef\]](#)

[25] Wu, A., & Ren, W. (2020). *TiO<sub>2</sub> nanoparticles: applications in nanobiotechnology and nanomedicine*. John Wiley & Sons.

[26] Gad, M. M., & Abualsaud, R. (2019). Behavior of PMMA denture base materials containing titanium dioxide nanoparticles. A literature review. *International Journal of Biomaterials*, 2019(1), 6190610. [\[CrossRef\]](#)

[27] Çeşmeli, S., & Avci, C. B. (2019). Application of titanium dioxide (TiO<sub>2</sub>) nanoparticles in cancer therapies. *Journal of Drug Targeting*, 27(7), 762-766. [\[CrossRef\]](#)

[28] Samrot, A. V., Angalene, J. L. A., Roshini, S. M., Stefi, S. M., Preethi, R., & Raji, P. (2022). Nanoparticles, a double-edged sword with oxidant as well as antioxidant properties—a review. *Oxygen*, 2(4), 591-604. [\[CrossRef\]](#)

[29] Buraso, W., Lachom, V., Siriya, P., & Laokul, P. (2018). Synthesis of TiO<sub>2</sub> nanoparticles via a simple precipitation method and photocatalytic performance. *Materials Research Express*, 5(11), 115003. [\[CrossRef\]](#)

[30] Sadek, O., Touhtouh, S., Rkhis, M., Anoua, R., El Jouad, M., Belhora, F., & Hajjaji, A. (2022). Synthesis by sol-gel method and characterization of nano-TiO<sub>2</sub> powders. *Materials Today: Proceedings*, 66, 456-458. [\[CrossRef\]](#)

[31] Arthi, G., Kavitha, B., & Palanisamy, P. K. (2023).

Solvothermal synthesis of 3D hierarchical rutile TiO<sub>2</sub> nanostructures for efficient dye-sensitized solar cells. *Materials Letters*, 337, 133961. [CrossRef]

[32] Ansari, A., Siddiqui, V. U., Rehman, W. U., Akram, M. K., Siddiqui, W. A., Alosaimi, A. M., ... & Rafatullah, M. (2022). Green synthesis of TiO<sub>2</sub> nanoparticles using Acorus calamus leaf extract and evaluating its photocatalytic and in vitro antimicrobial activity. *Catalysts*, 12(2), 181. [CrossRef]

[33] Aravind, M., Amalanathan, M., & Mary, M. S. M. (2021). Synthesis of TiO<sub>2</sub> nanoparticles by chemical and green synthesis methods and their multifaceted properties. *SN Applied Sciences*, 3(4), 409. [CrossRef]

[34] Chouke, P. B., Potbhare, A. K., Bhusari, G. S., Mondal, A., Chaudhary, R. G., & Meshram, N. P. (2019). Green fabrication of zinc oxide nanospheres by Aspidopterys cordata for effective antioxidant and antibacterial activity. *Advanced Materials Letters*, 10(5), 355-360. [CrossRef]

[35] Potbhare, A. K., Chaudhary, R. G., Chouke, P. B., Yerpude, S., Mondal, A., & Meshram, N. P. (2020). Rhizoctonia solani assisted biosynthesis of silver nanoparticles for antibacterial assay. *Materials Today: Proceedings*, 29, 939-945. [CrossRef]

[36] Venkatappa, M. M., Dandin, C. J., Shivakumar, H. R., Thippeswamy, B., & Shivanna, S. (2023). Green synthesised TiO<sub>2</sub> nanoparticles-mediated Terenna asiatica: evaluation of their role in reducing oxidative stress, inflammation and human breast cancer proliferation. *Molecules*, 28(13), 5126. [CrossRef]

[37] Peng, Y., Ao, M., Dong, B., Jiang, Y., Yu, L., Chen, Z., ... & Xu, R. (2021). Anti-inflammatory effects of curcumin in the inflammatory diseases: status, limitations and countermeasures. *Drug Design, Development and Therapy*, 15, 4503-4525. [CrossRef]

[38] Abouzid, M. R., Ali, K., Elnahass, Y. H., & Senousy, M. M. (2022). An overview of diabetes mellitus in Egypt and the significance of integrating preventive cardiology in diabetes management. *Cureus*, 14(7), e27290. [CrossRef]

[39] Jwad, S. M., & Al-Fatlawi, H. Y. (2022). Types of diabetes and their effect on the immune system. *Journal of Advances in Pharmacy Practice*, 4(1), 21-30.

[40] Abduh, N. A., Al-Senani, G. M., Al-Kadhi, N. S., Almaghrabi, O. A., Alshammari, N. K., & Abduh, M. S. (2025). Green synthesis of Zn-doped TiO<sub>2</sub> nanomaterials for photocatalytic degradation of crystal violet and methylene blue dyes under sunlight. *Biomass Conversion and Biorefinery*, 15(3), 4849-4865. [CrossRef]

[41] Preuss, H. G. (1997). Effects of glucose/insulin perturbations on aging and chronic disorders of aging: the evidence. *Journal of the American College of Nutrition*, 16(5), 397-403. [CrossRef]

[42] Yao, M., Li, Y., Wang, H., Shen, H., & Wang, Y. (2023). Projected burden of stroke in China through 2050. *Chinese Medical Journal*, 136(13), 1598-1605. [CrossRef]

[43] Hashmat, I., Azad, H., & Ahmed, A. (2012). Neem (*Azadirachta indica* A. Juss)-A nature's drugstore: an overview. *International Research Journal of Biological Sciences*, 1(6), 76-79.

[44] Paul, R., Prasad, M., & Sah, N. K. (2011). Anticancer biology of *Azadirachta indica* L (neem): a mini review. *Cancer Biology & Therapy*, 12(6), 467-476. [CrossRef]

[45] Shekhar, S., Sharma, S., Kumar, A., & Sharma, B. (2023). Green chemistry based benign approach for the synthesis of titanium oxide nanoparticles using extracts of *Azadirachta indica*. *Cleaner Engineering and Technology*, 13, 100607. [CrossRef]

[46] Sun, Y., Wang, S., & Zheng, J. (2019). Biosynthesis of TiO<sub>2</sub> nanoparticles and their application for treatment of brain injury-An in-vitro toxicity study towards central nervous system. *Journal of Photochemistry and Photobiology B: Biology*, 194, 1-5. [CrossRef]

[47] Maheshna, N., Kumar, R., Singh, S., & Sharma, A. (2022). Green synthesis of titanium dioxide nanoparticles and their multifaceted applications. *International Journal of Health Sciences*, 6(S2), 12515-12526. [CrossRef]

[48] Tasisa, Y. E., Sarma, T. K., Krishnaraj, R., & Sarma, S. (2024). Band gap engineering of titanium dioxide (TiO<sub>2</sub>) nanoparticles prepared via green route and its visible light driven for environmental remediation. *Results in Chemistry*, 11, 101850. [CrossRef]

[49] Ullah, A. M. A., Tamanna, A. N., Hossain, A., Akter, M., Kabir, M. F., Tareq, A. R. M., ... & Khan, M. N. I. (2019). In vitro cytotoxicity and antibiotic application of green route surface modified ferromagnetic TiO<sub>2</sub> nanoparticles. *RSC advances*, 9(23), 13254-13262. [CrossRef]

[50] Subapriya, R., & Nagini, S. (2005). Medicinal properties of neem leaves: a review. *Current Medicinal Chemistry-Anti-Cancer Agents*, 5(2), 149-156. [CrossRef]

[51] Zhu, X., Zhang, J., Chen, F., & Wang, L. (2021). Preparation and characterization of Cu-doped TiO<sub>2</sub> nanomaterials with anatase/rutile/brookite triphasic structure and their photocatalytic activity. *Journal of Materials Science: Materials in Electronics*, 32(17), 21511-21524. [CrossRef]

[52] Ganapathy, K., Rastogi, V., Lora, C. P., Suriyaprakash, J., Alarfaj, A. A., Hirad, A. H., & Indumathi, T. (2024). Biogenic synthesis of dopamine/carboxymethyl cellulose/TiO<sub>2</sub> nanoparticles using Psidium guajava leaf extract with enhanced antimicrobial and anticancer activities. *Bioprocess and Biosystems Engineering*, 47(1), 131-143. [CrossRef]

[53] Karmakar, S., Kumar, S., Rana, L., & Sharma, R. (2017). Optical properties of TiO<sub>2</sub>@C nanocomposites: synthesized by green synthesis technique. *Materials Letters*, 8(4), 449-457. [CrossRef]

[54] Muthuvel, A., Said, N. M., Jothibas, M., Gurushankar,

K., & Mohana, V. (2021). Microwave-assisted green synthesis of nanoscaled titanium oxide: photocatalyst, antibacterial and antioxidant properties. *Journal of Materials Science: Materials in Electronics*, 32(18), 23522-23539. [\[CrossRef\]](#)

[55] Verma, V., Al-Dossari, M., Singh, J., & Chauhan, P. (2022). A Review on Green Synthesis of TiO<sub>2</sub> NPs: Photocatalysis and Antimicrobial Applications. *Polymers*, 14(7), 1444. [\[CrossRef\]](#)

[56] Sellami, H., Khettaf, S., Boumaza, S., & Chaalal, O. (2025). Structural and optical characterization of TiO<sub>2</sub> nanoparticles synthesized using Globularia alypum leaf extract and the antibacterial properties. *Discover Applied Sciences*, 7(8), 834. [\[CrossRef\]](#)

[57] Shakeel, N., Piwoński, I., Iqbal, P., & Kisielewska, A. (2025). Green Synthesis of Titanium Dioxide Nanoparticles: Physicochemical Characterization and Applications: A Review. *International Journal of Molecular Sciences*, 26(12), 5454. [\[CrossRef\]](#)

[58] Bhatti, A., Sharma, R., Singh, P., & Kumar, V. (2025). Synergistic Effect of TiO<sub>2</sub>-Nanoparticles and Plant Growth-Promoting Microorganisms on the Physiological Parameters and Antioxidant Responses of Capsicum annum Cultivars. *Antioxidants*, 14(1), 89. [\[CrossRef\]](#)

[59] Al-darwesh, M. Y., Al-Kadhi, N. S., Al-Senani, G. M., & Abduh, N. A. (2025). Antimicrobial, anti-inflammatory, and anticancer potential of green synthesis TiO<sub>2</sub> nanoparticles using Sophora flavescens root extract. *Chemical Papers*, 79(2), 1207-1221. [\[CrossRef\]](#)

[60] Li, D., Li, L., Guo, W., Chang, Z., & Lu, M. (2015). Synthesis and characterization of Mo-Sb-S tridoped TiO<sub>2</sub> nanoparticles with enhanced visible light photocatalytic activity. *Materials Science in Semiconductor Processing*, 31, 530-535. [\[CrossRef\]](#)

[61] Nga, N. T. A., & Alahmadi, T. A. (2024). Assessment of possible biomedical applications of green synthesized TiO<sub>2</sub>NPs-an in-vitro approach. *Environmental Research*, 248, 118278. [\[CrossRef\]](#)

[62] Moaty, A. A. A., El-Kholie, E. A., & Adarous, R. A. (2022). The Anti-Diabetic Effect of Neem Leaves (Azadirachta indica,) in Alloxan-Induced Diabetic Rats. *Journal of Home Economics*, 32(2), 19-31.

[63] Tunkaew, K., Liewhiran, C., & Vaddhanaphuti, C. S. (2024). Functionalized metal oxide nanoparticles: A promising intervention against major health burden of diseases. *Life Sciences*, 358, 123154. [\[CrossRef\]](#)

[64] Shehadeh, M. B., Suaifan, G. A., & Abu-Odeh, A. M. (2021). Plants secondary metabolites as blood glucose-lowering molecules. *Molecules*, 26(14), 4333. [\[CrossRef\]](#)

[65] Allahverdiyev, A. M., Abamor, E. S., Bagirova, M., & Rafailovich, M. (2011). Antimicrobial effects of TiO<sub>2</sub> and Ag<sub>2</sub>O nanoparticles against drug-resistant bacteria and leishmania parasites. *Future Microbiology*, 6(8), 933-940. [\[CrossRef\]](#)

[66] Khater, M. S., Osman, M. S., & Hassan, A. A. (2020). Study to elucidate effect of titanium dioxide nanoparticles on bacterial membrane potential and membrane permeability. *Materials Research Express*, 7(3), 035005. [\[CrossRef\]](#)

[67] Pandya, P., & Ghosh, S. (2024). Biogenic TiO<sub>2</sub> Nanoparticles for Advanced Antimicrobial and Antiviral Applications. In V. Kokkarachedu & R. Sadiku (Eds.), *Nanoparticles in Modern Antimicrobial and Antiviral Applications* (pp. 151-174). Springer International Publishing. [\[CrossRef\]](#)

[68] Anandgaonker, P., Kulkarni, G., Gaikwad, S., & Rajbhoj, A. (2019). Synthesis of TiO<sub>2</sub> nanoparticles by electrochemical method and their antibacterial application. *Arabian Journal of Chemistry*, 12(8), 1815-1822. [\[CrossRef\]](#)

[69] Hussein, E. M., Desoky, W. M., Hanafy, M. F., & Guirguis, O. W. (2021). Effect of TiO<sub>2</sub> nanoparticles on the structural configurations and thermal, mechanical, and optical properties of chitosan/TiO<sub>2</sub> nanoparticle composites. *Journal of Physics and Chemistry of Solids*, 152, 109983. [\[CrossRef\]](#)

[70] Albukhaty, S., Naderi-Manesh, H., & Tiraihi, T. (2022). Preparation and characterization of titanium dioxide nanoparticles and in vitro investigation of their cytotoxicity and antibacterial activity against *Staphylococcus aureus* and *Escherichia coli*. *Animal Biotechnology*, 33(5), 864-870. [\[CrossRef\]](#)

[71] Thakur, B. K., Kumar, A., & Kumar, D. (2019). Green synthesis of titanium dioxide nanoparticles using Azadirachta indica leaf extract and evaluation of their antibacterial activity. *South African Journal of Botany*, 124, 223-227. [\[CrossRef\]](#)

[72] Santhoshkumar, T., Rahuman, A. A., Jayaseelan, C., Rajakumar, G., Marimuthu, S., Kirthi, A. V., ... & Kim, S. K. (2014). Green synthesis of titanium dioxide nanoparticles using Psidium guajava extract and its antibacterial and antioxidant properties. *Asian Pacific Journal of Tropical Medicine*, 7(12), 968-976. [\[CrossRef\]](#)

[73] Arora, B., Murar, M., & Dhumale, V. (2015). Antimicrobial potential of TiO<sub>2</sub> nanoparticles against MDR *Pseudomonas aeruginosa*. *Journal of Experimental Nanoscience*, 10(11), 819-827. [\[CrossRef\]](#)

**Sidra Mamoor** received her MPhil degree in Physics from Abdul Wali Khan University Mardan, Khyber Pakhtunkhwa, Pakistan, in 2025. (Email: sidramamoorthy@gmail.com)

**Atta Ullah** received his BS degree in Physics from Abdul Wali Khan University Mardan, Khyber Pakhtunkhwa, Pakistan, in 2024. He is currently pursuing his MPhil degree from the same university. His research interests include Metal-Organic Frameworks, Prussian Blue Analogues for energy storage and biomedical applications, and perovskite solar cells. (Email: khanattaullah052@gmail.com)

**Sulaiman Khan** received his MPhil degree in Physics from Abdul Wali Khan University Mardan, Khyber Pakhtunkhwa, Pakistan, in 2025. (Email: [sulaimanhamdard10@gmail.com](mailto:sulaimanhamdard10@gmail.com))

**Waleed Ahsan Akber** received his MPhil degree in Physics from Abdul Wali Khan University Mardan, Khyber Pakhtunkhwa, Pakistan, in 2022. His research interests include metal oxide semiconductors for biomedical and solar cell applications. (Email: [smwaleedkhan@gmail.com](mailto:smwaleedkhan@gmail.com))

**Shakir Ali** received his MPhil degree in Zoology by Physics from Abdul Wali Khan University Mardan, Khyber Pakhtunkhwa, Pakistan, in 2022. He is currently pursuing his PhD in Zoology by Physics from the same university. His research focuses on oxide nanostructures for biomedical applications. (Email: [shakirali4008@gmail.com](mailto:shakirali4008@gmail.com))

**Adil Sher** received his MPhil degree in Zoology from Abdul Wali Khan University Mardan, Khyber Pakhtunkhwa, Pakistan, in 2022. He is currently pursuing his PhD in Zoology from the same university. His research focuses on oxide nanostructures for biomedical applications. (Email: [adilsher@awkum.edu.pk](mailto:adilsher@awkum.edu.pk))

**Gauhar Rehman** is a Professor of Zoology at Abdul Wali Khan University Mardan, Khyber Pakhtunkhwa, Pakistan. He received his PhD degree in Zoology from South Korea in 2012. His research interests include animal physiology, biodiversity, and environmental biology, with numerous publications on regional fauna and ecological conservation. (Email: [gauhar@awkum.edu.pk](mailto:gauhar@awkum.edu.pk))

**Khizar Hayat** is an Associate Professor of Physics at Abdul Wali Khan University Mardan, Khyber Pakhtunkhwa, Pakistan. He received his PhD from PIEAS Islamabad in 2014 and completed postdoctoral research in China in 2018. His research interests include condensed matter physics, nanomaterials, and optoelectronic devices. (Email: [khizar3@awkum.edu.pk](mailto:khizar3@awkum.edu.pk))

**Said Karim Shah** is a Professor of Physics at Abdul Wali Khan University Mardan, Khyber Pakhtunkhwa, Pakistan. He earned his PhD from the University of Camerino, Italy, in 2012 and completed postdoctoral research at the Institute Polytechnique de Bordeaux, France, in 2014. His research interests include  $TiO_2$  and  $ZnO$  nanostructures, solar cells, and organic-inorganic semiconductor devices. With over 55 international publications, he has secured multiple HEC-NRPU research grants. He is also an HEC-approved PhD supervisor, actively mentoring BS, MPhil, and PhD students. (Email: [saidkarim@awkum.edu.pk](mailto:saidkarim@awkum.edu.pk))